Coordination States of Molybdenum and the Nature of Copper Ion Sites in the Superionic Glasses xCuI·$(1 - x)$$Cu_2MoO_4$ ($x = 0.4, 0.5$) Studied by Infrared Reflectance Spectroscopy

C. P. Varsamis and E. I. Kamitsos*

Theoretical and Physical Chemistry Institute, National Hellenic Research Foundation, 48 Vass. Constantinou Ave., Athens 116 35, Greece

N. Machida

Department of Chemistry, Konan University, 8-9-1 Okamoto, Higashinada-ku, Kobe 658, Japan

T. Minami

College of Engineering, Osaka Prefecture University, 1-1 Gakuen-chu, Sakai, Osaka 593, Japan

Received: January 30, 1997[⊗]

The reflectance spectra of the superionic glasses xCuI·$(1 - x)$$Cu_2MoO_4$ ($x = 0.4, 0.5$) have been measured in the mid- and far-infrared range to investigate the structure of the oxyanion matrix and the nature of sites hosting the charge carrier copper ions. The analysis of the mid-infrared spectra revealed the presence of three types of molybdate polyhedra: MoO_4^{2-} monomers (the majority units), $Mo_2O_7^{2-}$ dimers (minority units), and MoO_6^{6-} isolated octahedra (minority units). The presence of $MoO_{4/2}O_2^{2-}$ type octahedra, which contain four bridging and two nonbridging oxygen atoms, was excluded on the basis of the spectroscopic results. The relative abundance of the three types of molybdate structural units was found to depend on the glass transition temperature, T_g; the equilibrium between these molybdate units shifts toward dimers and octahedra upon decreasing T_g. This is effected by increasing the mole fraction of CuI in the glass. Thus, CuI affects indirectly the glass structure by lowering the temperature at which the structure of the supercooled liquid is frozen into the glassy state. The study of the far-infrared profiles has suggested that the cuprous ions exist in three coordination environments; two of these are formed by oxygen atoms provided by the oxyanion matrix and the third is formed primarily by iodide anions. The vibrational characteristics of such CuI-like environments suggest their disordered nature with respect to crystalline CuI. The findings of this work are in agreement with the results of our previous investigations on analogous AgI-containing glasses and lends support to the conduction pathway model proposed for ion transport in such superionic glasses. Calculation of effective charges on the basis of the far-infrared data indicated that copper is present in the +1 oxidation state in these glasses.

1. Introduction

Superionic glasses have attracted much attention for fundamental studies of the ion transport mechanism and for their technological applications in electrochemical devices.[1−4] Among them, the AgI-containing glasses have been extensively investigated as model glassy ionic conductors because of their high ionic conductivity at room temperature (in the range of 10^{-1} to 10^{0} S m^{-1}). Despite the numerous studies devoted to such model systems the identification of the structures responsible for high ionic conductivity leaves some problems still under investigation.[2,5]

In recent years, new superionic glass compositions were prepared in the systems xCuX·$(1 - x)$[Cu_2O·A_xO_y], where X = I, Br, Cl and the Lewis acid A_xO_y is P_2O_5, MoO_3, WO_3, or combinations of these oxides.[6−12] Such Cu^+ ion conducting glasses exhibit conductivities which are comparable, or even higher in some cases than the conductivities of the known silver analogues.[13] However, only a few works have been reported so far on the structural aspects of the new Cu^+ glassy conductors in comparison to the widely investigated Ag^+-containing glasses.

For the particular case of glasses in the pseudobinary system xCuI·$(1 - x)$$Cu_2MoO_4$ the existing structural evidence is highly contradictory. On the basis of mid-infrared transmission spectra Machida et al.[8,10] concluded that these glasses are fully ionic, since they are composed of Cu^+, I^-, and MoO_4^{2-} tetrahedral ions. On the other hand, Saito et al.[14] interpreted the results of anomalous X-ray scattering study of the $x = 0.46$ glass as suggesting a three-dimensional network structure based on corner-sharing MoO_6 octahedral units.

In an attempt to resolve the above controversies we have performed an infrared reflectance study of the $x = 0.4$ and 0.5 glasses in the xCuI·$(1 - x)$$Cu_2MoO_4$ family. This technique was chosen because it leads to true band shapes and intensities,[15,16] while spectra measured by transmission of powdered glass dispersed in a matrix material may suffer from considerable distortions of band shapes and nonreproducible intensities of absorption bands. Vibrations of the local polyhedra of glass forming cations give rise to intense bands observed mainly in the mid-infrared range. Therefore, appropriate analysis of the mid-infrared spectra is expected to give information on the coordination state of molybdenum atoms, as well as on the influence that CuI may have on the glass structure. The nature of the coordination environments of the glass modifying cations, i.e., Cu^+ in this case, can be deduced from the analysis of the localized cation motions active in the far-infrared.[15,16] Such information is particularly valuable in discussing the merits of the various models proposed for ion transport in glass.[1−3]

* Corresponding author. Tel: +30-1 724 9483. Telefax: +30-1 724 9104. E-mail: eik@apollon.servicenet.ariadne-t.gr.

[⊗] Abstract published in *Advance ACS Abstracts,* April 15, 1997.

S1089-5647(97)00373-8 CCC: $14.00

Recent far-infrared studies of glasses in the systems xAgI·$(1 - x)$[Ag_2O·nM_xO_y], where $M_xO_y = P_2O_5$, MoO_3, or B_2O_3, have suggested that Ag^+ ions occupy three types of site; one provided by iodide anions and the other two formed primarily by oxygen atoms.[17,18] The extent of aggregation of the silver iodide clusters into disordered AgI microdomains was found to increase with AgI content and to depend on the nature of the oxyanion host matrix. In view of these findings, and the continuing search for establishing a common ion transport mechanism in superionic glasses, it is of interest to investigate whether CuI in the glass matrix behaves in a similar manner.

The synthesis of Cu^+ ion conducting glasses has been restricted so far in limited glass-forming systems. This is in contrast to the Ag^+-containing glasses which have been obtained in many systems, including those based on strong glass forming oxides such as SiO_2 and GeO_2.[13] The reason for this restriction is related to the easy oxidation of Cu^+ ion to Cu^{2+} and/or its disproportionation to Cu^0 and Cu^{2+} during melting.[7,8,11,19] To eliminate these problems, special care has been exercised during the glass-forming process. In addition, the reflectance data in the far-infrared have been employed to estimate the effective charge of Cu ions, allowing therefore the determination of the formal oxidation state of copper in the glasses under investigation.

2. Experimental Section

2.1. Glass Preparation. Glasses were prepared from reagent-grade CuI, Cu_2O, and MoO_3. Stoichiometric amounts of the dry reagents were thoroughly mixed in a glovebox filled with dry nitrogen gas and melted in silica glass tubes under nitrogen (1 atm) at 500 °C for 3 h, and then quenched in ice water. This preparation technique results in xCuI·$(1 - x)$$Cu_2MoO_4$ glasses with $0.35 \leq x \leq 0.55$,[8-10] but only the compositions with $x = 0.4$ and $x = 0.5$ were investigated here because these are the ones well within the glass-forming region.

The silica tubes containing the glasses were cut, using a low-speed diamond saw, to remove glass plates of approximate dimensions $0.8 \times 0.8 \times 0.3$ cm^3. These specimens were subsequently polished for infrared measurements.

2.2. Infrared Measurements. Infrared spectra were measured at room temperature on a Fourier-transform vacuum spectrometer (Bruker 113v), properly equipped with sources, detectors, and beamsplitters to allow a continuous coverage in the 25−5000 cm^{-1} range. Specular reflectance measurements were made in a quasi-normal incidence mode (11°), using an aluminum mirror as reference. Each spectrum is the average of 200 scans at 2 cm^{-1} resolution.

2.3. Analysis of Infrared Data. The experimental infrared data have been analyzed by two different procedures: (a) deconvolution of absorption coefficient spectra, which were calculated directly through the Kramers−Kronig analysis of the reflectance data without reference to any model, and (b) reflectance curve fitting using the classical dispersion theory to model the dielectric function. Details concerning the first procedure can be found elsewhere,[15,16] while a brief description of the theory used for reflectance curve fitting is given below.

In general, the reflectance of a sample of finite thickness is given by a complex expression which accounts for multiple internal reflections. However, in the case of an absorbing medium with negligible transmittance only the contribution of the first interface has to be considered and the reflectance, $R(\nu)$, at normal incidence is given by[20]

$$R(\nu) = \frac{[n(\nu) - 1]^2 + k^2(\nu)}{[n(\nu) + 1]^2 + k^2(\nu)} \quad (1)$$

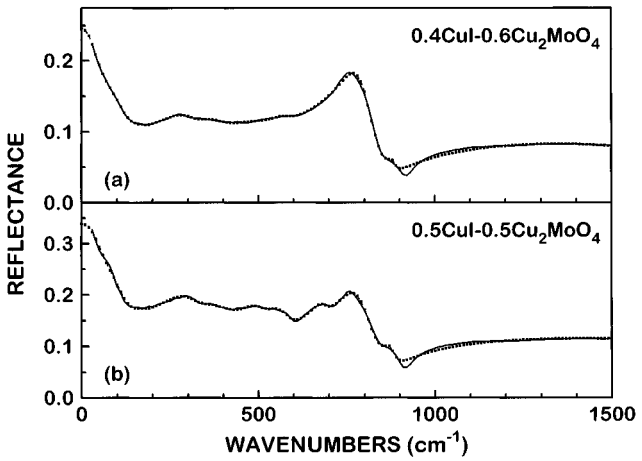

Figure 1. Infrared reflectance spectra of xCuI·$(1 - x)$$Cu_2MoO_4$ glasses. Solid lines indicate the measured spectra. The dotted lines are the best fit of eq 3 to reflectivity data.

In the above expression, $n(\nu)$ and $k(\nu)$ are the real and imaginary part, respectively, of the complex refractive index, $\tilde{n}(\nu)$, which is related to the complex dielectric function, $\tilde{\epsilon}(\nu)$, through the expression:

$$\tilde{n}(\nu) \equiv n(\nu) + ik(\nu) = \sqrt{\tilde{\epsilon}(\nu)} \quad (2)$$

The complex dielectric function $\tilde{\epsilon}(\nu)$ of the glass is modeled here according to the classical dispersion theory[21,22] as follows:

$$\tilde{\epsilon}(\nu) = \epsilon'(\nu) + i\epsilon''(\nu) = \epsilon_\infty + \sum_j \frac{\Delta\epsilon_j \nu_j^2}{\nu_j^2 - \nu^2 - i\nu\Gamma_j} \quad (3)$$

where the summation is over j Lorentzian oscillators, each one characterized by the resonance frequency ν_j the bandwidth Γ_j and the dielectric strength $\Delta\epsilon_j$, and ϵ_∞ is the high-frequency dielectric constant. Combination of eqs 2 and 3 yields the following expressions for the real and imaginary parts of the dielectric function and the refractive index, in terms of the model

$$\epsilon'(\nu) = n^2(\nu) - k^2(\nu) = \epsilon_\infty + \sum_j \frac{\Delta\epsilon_j \nu_j^2(\nu_j^2 - \nu^2)}{(\nu_j^2 - \nu^2)^2 + \Gamma_j^2\nu^2} \quad (4)$$

$$\epsilon''(\nu) = 2n(\nu)k(\nu) = \sum_j \frac{\Delta\epsilon_j \nu_j^2 \Gamma_j \nu}{(\nu_j^2 - \nu^2)^2 + \Gamma_j^2\nu^2} \quad (5)$$

The characteristic parameters of each oscillator (ν_j, Γ_j, $\Delta\epsilon_j$) and the high-frequency dielectric constant, ϵ_∞, are the adjustable parameters. They are determined by best-fitting the reflectance calculated from eqs 1, 4, and 5 to the experimental reflectivity spectrum. If there is no dispersion of the dielectric constant for frequencies below the far-infrared range, then the static dielectric constant of the material, $\epsilon_0 \equiv \epsilon'(\nu{=}0)$, can be obtained from the expression

$$\epsilon_0 = \epsilon_\infty + \sum_j \Delta\epsilon_j \quad (6)$$

where the contribution of the dielectric strength of all oscillators has been considered.

3. Results

The infrared reflectance spectra of the $x = 0.4$ and $x = 0.5$ glasses are shown in Figure 1. To the best of our knowledge,

TABLE 1: Dispersion Parameters Obtained by Fitting Eq 3 to Reflectivity Data of xCuI·$(1-x)$$Cu_2MoO_4$ Glasses

	0.4CuI·0.6Cu_2MoO_4			0.5CuI·0.5Cu_2MoO_4		
j	ν_j (cm^{-1})	Γ_j (cm^{-1})	$\Delta\epsilon_j$	ν_j (cm^{-1})	Γ_j (cm^{-1})	$\Delta\epsilon_j$
1	58.0	110.0	3.422	62.8	110.0	6.254
2	113.8	115.0	1.029	110.0	112.1	1.662
3	175.0	50.0	0.025	180.0	50.0	0.043
4	301.0	90.0	0.109	310.0	113.7	0.430
5	390.0	144.6	0.161	399.4	145.2	0.394
6	490.0	100.0	0.048	501.9	91.2	0.167
7	579.2	79.9	0.034	570.3	88.3	0.192
8	670.0	70.0	0.010	684.4	58.2	0.077
9	782.5	104.8	0.441	779.0	110.7	0.500
10	881.5	30.3	0.011	875.1	40.0	0.027
		$\epsilon_\infty = 3.4$			$\epsilon_\infty = 4.4$	

far-infrared spectra of Cu^+-containing glasses are reported for the first time in this work. Even though the measured reflectance curves are quite similar, characteristic differences may be noted. Increasing the CuI content appears to result in a higher reflectivity amplitude in the far-IR region and a more structured reflectivity profile at higher frequencies.

In modeling the complex dielectric function $\tilde{\epsilon}(\nu)$ according to eq 3 the minimum number of oscillators that give a satisfactory description of the experimental reflectivity has been utilized. Thus, it was found that 10 oscillators could be used to fit the data. The comparison between experimental and fitted reflectivity shows good agreement as evidenced in Figure 1. The dispersion parameters obtained by fitting the reflectivity data are given in Table 1. The accuracy in determining the resonance frequency is ± 2 cm^{-1} for the strongest modes and ± 5 cm^{-1} for the weak ones. The corresponding accuracies for the line widths are ± 5 and ± 10 cm^{-1}, respectively, while the oscillator strength values are accurate to $\pm 2\%$ and $\pm 8\%$, respectively. Considering that each reflectivity spectrum results from broad and strongly overlapping reflectivity peaks, the results in Table 1 show that, within experimental error, the resonance frequency and line width of each oscillator are very little affected by increasing the CuI content. Nevertheless, it is clear that the relative dielectric strengths of the oscillators change with CuI content. It is noted here that, although the dielectric function is modeled as a sum of independent Lorentzian components, the resulting reflectance fitting function is a complex combination of the Lorentzian components.

The absorption coefficient spectra calculated by the Kramers−Kronig relations are shown in Figure 2. As in the case of reflectivity, these spectra were deconvoluted into 10 component bands. It was found though that the absorption coefficient spectra could be best described by a sum of Gaussian profiles:

$$\alpha(\nu) = \sum_j \alpha_j e^{-2(\nu-\nu_j)^2/\Delta\nu_j^2} \qquad (7)$$

Each Gaussian component is characterized by a resonance frequency, ν_j, a bandwidth, $\Delta\nu_j$, and the value of the absorption coefficient at the resonance frequency, α_j. Note that $\sqrt{2}\Delta\nu_j$ gives the full width at 1/e of the maximum absorption. The integrated intensity, $\langle A\rangle_j$, of the j-th Gaussian component can be easily calculated by

$$\langle A\rangle_j \equiv \int_{-\infty}^{\infty} \alpha_j e^{-2(\nu-\nu_j)^2/\Delta\nu_j^2}\, d\nu = \sqrt{\pi/2}\Delta\nu_j\alpha_j \qquad (8)$$

The deconvolution parameters, as well as the integrated intensities, of the resulted bands are reported in Table 2. The experimental errors in determining ν_j and $\Delta\nu_j$ are similar to those of the reflectivity fitting procedure, while the error of the integrated intensity is $\pm 3\%$ for the strongest bands and $\pm 7\%$ for the weak ones.

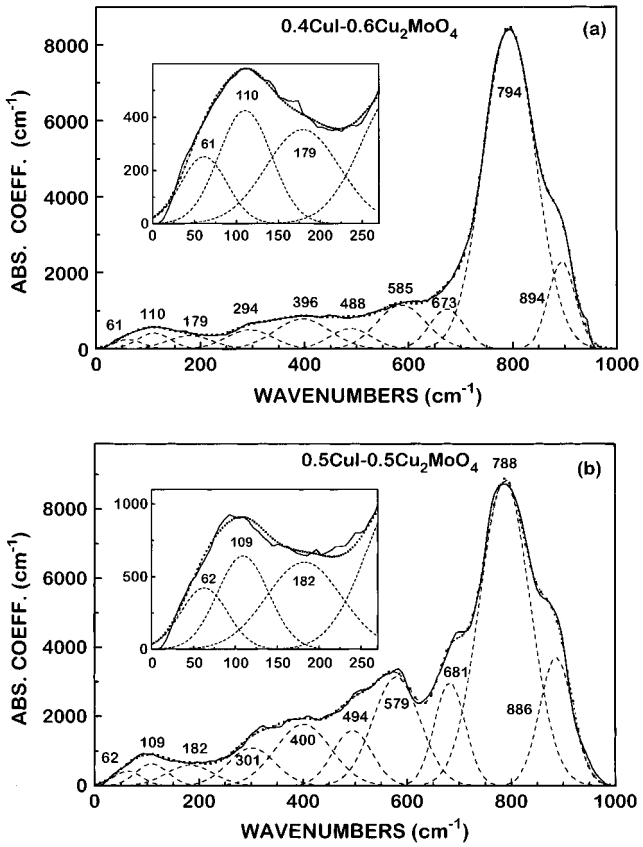

Figure 2. Absorption coefficient spectra (solid lines) of xCuI·$(1-x)$$Cu_2MoO_4$ glasses obtained by Kramers−Kronig analysis of the reflectivity spectra: (a) $x = 0.4$ and (b) $x = 0.5$. Deconvoluted Gaussian component bands and simulated spectra are shown by dashed and dotted lines, respectively. The insets show in an expanded scale the comparison of experimental and simulated far-infrared spectra.

Comparison of the results presented in Tables 1 and 2 shows that the values of resonance frequencies and bandwidths obtained from the reflectance and absorption analysis are quite similar. The main origin of the small discrepancies observed can be traced to the different fitting function utilized. While the reflectance is fitted classically with Lorentzian band shapes (eq 3), the absorption coefficient spectra were found to be best fitted by a sum of Gaussian profiles. This is in agreement with results of previous studies on oxide and chalcogenide glasses which have shown that infrared absorption and Raman scattering bands are best fitted with Gaussian rather than Lorentzian line shapes.[15,23−25] We note also that the absorption coefficient, $\alpha(\nu)$, depends only on the extinction coefficient $k(\nu)$, i.e., $\alpha(\nu) = 4\pi\nu k(\nu)$, while the dielectric function $\tilde{\epsilon}(\nu)$ depends on both $n(\nu)$ and $k(\nu)$. Thus, the dispersion of $n(\nu)$ influences only the reflectance fitting procedure.

The fact that the two procedures used to analyze the data give very similar results is strengthened by the data presented in Figure 3. The optical ($n(\nu)$ and $k(\nu)$) and dielectric ($\epsilon'(\nu)$ and $\epsilon''(\nu)$) properties obtained by the Kramers−Kronig analysis and by the fitting procedure are compared in this figure for the $x = 0.5$ glass composition. It is clear that the results of the two methods of analysis are almost identical in a broad infrared range.

4. Discussion

4.1. Interpretation of Mid-Infrared Spectra. As noted in the Introduction, two different viewpoints have been expressed

TABLE 2: Deconvolution Parameters of the Absorption Coefficient Spectra of xCuI·(1 − x)Cu_2MoO_4 Glasses

	0.4CuI·0.6Cu_2MoO_4				0.5CuI·0.5Cu_2MoO_4			
j	ν_j (cm^{-1})	$\Delta\nu_j$ (cm^{-1})	α_j (cm^{-1})	$\langle A_j\rangle$ (10^4 cm^{-2})	ν_j (cm^{-1})	$\Delta\nu_j$ (cm^{-1})	α_j (cm^{-1})	$\langle A_j\rangle$ (10^4 cm^{-2})
1	61.0	55.0	252.5	1.74	62.5	55.6	425.1	2.96
2	110.1	63.0	425.9	3.36	109.0	61.3	645.0	4.95
3	179.0	88.2	353.7	3.91	182.0	89.9	602.1	6.78
4	294.3	89.1	509.6	5.69	301.0	90.0	1104.2	12.44
5	395.8	106.1	794.7	10.57	399.9	106.5	1783.2	23.80
6	488.1	79.8	544.5	5.44	494.3	74.5	1607.5	15.01
7	585.9	94.2	1159.7	13.70	579.2	91.1	3159.2	36.07
8	673.1	65.1	1059	8.64	681.0	58.5	3002	22.01
9	793.8	99.0	8484	105.27	788.0	96.9	8898.1	108.10
10	894.1	51.8	2307.9	14.98	886.1	63.1	3724.2	29.47

TABLE 3: Correlation Table for T_d and C_{3v} Point Group Symmetries of XY_4 Molecules and Infrared Frequencies (in cm^{-1}) of Molybdate Tetrahedra in Crystalline Compounds[a]

mode	T_d	C_{3v}	Li_2MoO_4[b]	$BaMoO_4$[c]	$CaMoO_4$[d]	$PbMoO_4$[d]
ν_1, ν_s(XY)	A_1(R)	A_1(R,IR)				
ν_3, ν_{as}(XY)	T_2(R,IR)	A_1(R,IR)+E(R,IR)	830 (s)	830 (s, b)	813	786
ν_2, δ(YXY)	E(R)	E(R,IR)	440 (s, b)	385 (m)	431	374
ν_4, δ(YXY)	T_2(R,IR)	A_1(R,IR)+E(R,IR)	370 (m)	335 (m)	329, 284	307, 272

[a] R and IR denote Raman and infrared activity, respectively. ν_s, ν_{as}, and δ designate symmetric stretching, asymmetric stretching, and bending modes, respectively. Relative intensities are indicated by s, strong; m, medium; w, weak; and b, broad. [b] Reference 28. [c] Reference 29. [d] Reference 30.

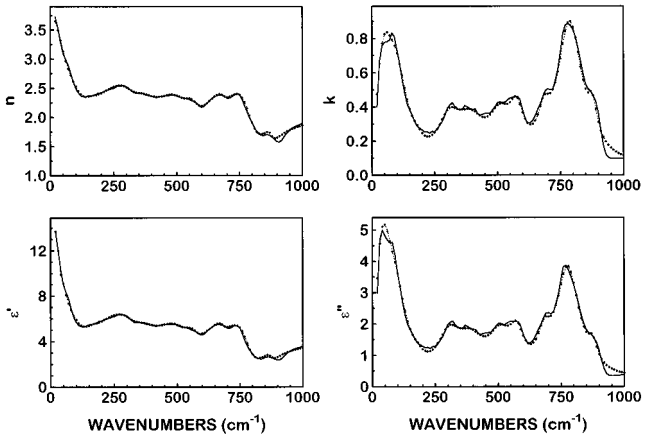

Figure 3. Comparison of optical (n,k) and dielectric (ϵ',ϵ'') properties obtained by the Kramers−Kronig analysis (full lines) and the fitting procedure (dotted lines). The data presented are for the 0.5CuI·0.5Cu_2-MoO_4 glass.

for the structural building units present in the glasses under investigation. According to Machida et al.,[8−10] molybdenum is fourfold coordinated, forming MoO_4^{2-} tetrahedra, with all oxygen atoms being nonbridging or terminal. Saito et al.[14] proposed that corner sharing MoO_6 octahedral units form the glass network. Therefore, in order to assign the infrared spectra measured in this work and discuss the glass structure it is essential to review briefly the predictions of group theory for the vibrational characteristics of tetrahedral and octahedral species and to consider reported infrared data for molybdates of known structure.

Perfect MoO_4^{2-} species will have the tetrahedral (T_d) point group symmetry. However, distortions of the molybdate tetrahedron due to differences in Mo−O bond lengths, a phenomenon encountered frequently in molybdates,[26] will result in reduction of T_d symmetry. In Table 3 T_d is correlated with C_{3v}, i.e., the symmetry of a distorted tetrahedron.[27] Despite the possibility of distortions, the main characteristic of the infrared spectra of molybdate compounds containing MoO_4^{2-} tetrahedra remains the strong band in the range 780−840 cm^{-1}.[28−30] This band is due to the asymmetric stretching mode of the Mo−O bond, ν_{as}(Mo−O), and its frequency depends on the type of the charge balancing cation.

TABLE 4: Correlation Table for O_h and D_{4h} Point Group Symmetries of XY_6 and XY_4Z_2 Molecules and Infrared Frequencies of Molybdate Octahedra in Crystalline Compounds[a]

XY_6 molecule O_h		XY_4Z_2 molecule D_{4h}		infrared frequencies (cm^{-1})	
mode	activity	activity	mode	$CoMoO_4$[b]	$NiMoO_4$[c]
ν_1, ν_s(XY)	A_{1g} (R)	A_{1g} (R)	ν_1, ν_s(XY)		
ν_2, ν_s(YXY)	E_g (R)	A_{1g} (R)	ν_{2a}, ν_s(XZ)		
		B_{1g} (R)	ν_{2b}, ν_s(XY)		
ν_3, ν_{as}(XY)	T_{1u} (IR)	A_{2u} (IR)	ν_{3a}, ν_{as}(XZ)	940 (s)	980 (s)
		E_u (IR)	ν_{3b}, ν_{as}(XY)	850 (m, sh), 775 (m)	960 (s), 935 (s)
ν_4, δ(YXY)	T_{1u} (IR)	A_{2u} (IR)	ν_{4a}, δ(ZYZ)	640 (m, b)	630 (s, b)
		E_u (IR)	ν_{4b}, δ(YXY)	420 (m, b)	445 (s, b)
ν_5, δ(YXY)	T_{2g} (R)	B_{2g} (R)	ν_{5a}, δ(ZYZ)		
		E_g (R)	ν_{5b}, δ(YXY)		
ν_6, δ(YXY)	T_{2u} (ia)	B_{2u} (ia)	ν_{6a}, δ(ZYZ)		
		E_u (IR)	ν_{6b}, δ(YXY)	295 (m), 255 (m, b)	375 (w), 355 (w)

[a] R, IR, and ia denote Raman active, infrared active, and inactive modes. ν_s, ν_{as}, and δ designate symmetric stretching, asymmetric stretching, and bending modes, respectively. Relative intensities are indicated by s, strong; m, medium; w, weak; b, broad; and sh, shoulder. [b] References 28 and 31. [c] Reference 29.

An octahedral XY_6 molecule with O_h symmetry exhibits six normal modes of vibration as shown in Table 4.[27] The asymmetric stretching mode, ν_3, and the ν_4 bending mode are the only ones active in the infrared. If molybdate octahedra are the species present in the glasses under investigation then they should obey the orthomolybdate (MoO_4^{2-}) stoichiometry. Octahedral species of the type $MoO_{4/2}O_2^{2-}$ which contain four bridging and two nonbridging oxygen atoms are isomeric to the MoO_4^{2-} tetrahedra;

$$MoO_{4/2}O_2^{2-} \rightleftarrows MoO_4^{2-} \qquad (9)$$

Creation of two nonbridging oxygen atoms in the $MoO_{6/2}$ octahedra reduces the point group symmetry from O_h to D_{4h} (i.e., XY_4Z_2 type molecule). The main manifestation of this in the infrared is the splitting of the ν_3 and the ν_4 modes into two components of A_{2u} and E_u symmetries (Table 4). Indeed, this was found to be the case of molybdate compounds like $CoMoO_4$[28,31] and $NiMoO_4$,[29] which contain the $MoO_{4/2}O_2^{2-}$ structural unit (Table 4). The strong band at high frequencies (940, 980 cm^{-1}) has been assigned to the asymmetric stretching of the Mo−O_t bonds ($O_t \equiv$ nonbridging oxygen), while infrared bands in the range 775−960 cm^{-1} are attributed to the corresponding Mo−O_b bonds, where $O_b \equiv$ bridging oxygen.[28,31] Therefore, the presence of $MoO_{4/2}O_2^{2-}$ octahedral units is manifested mainly by the strong infrared band at frequencies well above 900 cm^{-1}, due to the ν_{as}(Mo−O_t) mode.

Inspection of Tables 1 and 2 and Figure 2 shows that the infrared spectra of the $x = 0.4$ and 0.5 glasses exhibit the strongest feature at *ca*. 790 cm^{-1}, while the infrared activity above 900 cm^{-1} is weak. On the basis of the above discussion, these results strongly suggest that the existence of $MoO_{4/2}O_2^{2-}$ type octahedra in the $x = 0.4$ and 0.5 glasses should be excluded, at least in concentrations detectable by infrared spectroscopy. The strongest band at *ca*. 790 cm^{-1} can be attributed to the ν_3 mode of MoO_4^{2-} tetrahedra in agreement with the literature data presented in Table 3. The corresponding mode of MoO_4^{2-} tetrahedra in AgI-containing molybdate glasses was observed at 775 cm^{-1}.[18] The band at *ca*. 300 cm^{-1} can be attributed to a combined contribution of the ν_2 and ν_4 bending modes of molybdate tetrahedra.

Besides the above features which are characteristic of MoO_4^{2-} tetrahedra, the infrared spectra exhibit additional bands at *ca*. 400, 490, 580, 680, and 890 cm^{-1}. These features imply the existence of additional molybdate structures besides the majority of MoO_4^{2-} anions. In particular, the bands at *ca*. 490 and 580 cm^{-1} can be taken as suggesting the existence of $Mo_2O_7^{2-}$ dimers, since they can be attributed to the ν_s(Mo−O−Mo) and ν_{as}(Mo−O−Mo) stretching modes, respectively, of the Mo−O−Mo bridge of the dimers.[10,18,30,32] The high-frequency band at *ca*. 890 cm^{-1} can be assigned to the asymmetric stretching of the MoO_3^- units of $Mo_2O_7^{2-}$ dimers, ν_{as} (MoO_3^-), without excluding a small contribution from the infrared activation of the ν_1 mode of distorted MoO_4^{2-} tetrahedra in the glass.[18]

The bands at *ca*. 400 and 580 cm^{-1} can be assigned to the infrared active ν_4 and ν_3 modes of MoO_6^{6-} molybdate octahedra.[27] Crystalline Ba_2CaMoO_6, which contains isolated MoO_6^{6-} octahedra, shows ν_4 at 358 cm^{-1}, while ν_3 splits into two components at 600 and 648 cm^{-1}.[34] Similarly, the activity of MoO_6^{6-} octahedra in the infrared spectrum of Ba_2NiMoO_6[29] appears at 395 cm^{-1} (ν_4) and at 590 cm^{-1} and 650 cm^{-1} (ν_3). Besides the contribution of the ν_4 mode of MoO_6^{6-} octahedra, part of the intensity of the 400 cm^{-1} band can arise from the bending mode, $\delta(MoO_3^-)$, of the MoO_3^- units of the dimers.[33]

The spectral interpretations discussed above, and summarized in Table 5, show clearly that the structure of the oxyanion matrix can be described in terms of three different types of molybdate units: molybdate tetrahedra in the form of MoO_4^{2-} monomers and $Mo_2O_7^{2-}$ dimers, and molybdate octahedra in the form of isolated MoO_6^{6-} species. If the extinction coefficients of these species are not very different, then the results in Tables 1 and 2 suggest that the MoO_4^{2-} tetrahedra are the majority species. As suggested previously,[18] the minority molybdate species can result from a disproportionation of MoO_4^{2-} tetrahedra, such as

$$5MoO_4^{2-} \rightleftarrows MoO_6^{6-} + 2Mo_2O_7^{2-} \qquad (10)$$

In a recent study of silver iodomolybdate glasses, Pappin et al.[35] examined the effects of pressure and pressure vitrification on glass structure and properties. They found that the structure of glasses vitrified at high pressures (50 kbar) above the glass transition temperature can be described in terms of eq 10. The main difference between the pressure vitrified glasses and those prepared under normal quenching conditions was found to be the shift of eq 10 to the right in the former case. This was explained in terms of Le Chatelier's Principle, which predicts in this case the accelerated formation of dimers and octahedral molybdates as a means of absorbing the effects of pressure.[35]

TABLE 5: Assignments of Infrared Bands in the Absorption Spectrum of $0.5CuI \cdot 0.5Cu_2MoO_4$ Glass[a]

band frequency (cm^{-1})	assignments
886	$\nu_{as}(MoO_3^-) + \nu_1(MoO_4^{2-})$
788	$\nu_3(MoO_4^{2-})$
681	$\nu_3(MoO_6^{6-})$
579	ν_{as}(Mo−O−Mo)
494	ν_s(Mo−O−Mo)
400	$\nu_4(MoO_6^{6-}) + \delta(MoO_3^-)$
301	$\nu_2(MoO_4^{2-}) + \nu_4(MoO_4^{2-})$
182	ν(Cu−O)[+ rot(MoO_4^{2-}) + δ(Mo−O−Mo)]
109	ν(Cu−I)
62	ν(Cu−O)

[a] For details see text.

4.2. Effect of CuI on the Structure of the Oxyanion Matrix. It is observed in Figure 2 that the relative intensities of bands due to $Mo_2O_7^{2-}$ and MoO_6^{6-} species appear enhanced in the spectrum of the $x = 0.5$ glass, indicating that addition of CuI induces the shift of eq 10 to the right. In that respect, it is of interest to consider the results in Tables 1 and 2 and examine whether they are in accord with the predictions of eq 10. Following the assignments in Table 5, we take as characteristic of MoO_4^{2-} tetrahedra the sum of the contributions of bands at *ca*. 790 and 300 cm^{-1}. The contribution of $\nu_1(MoO_4^{2-})$ to the *ca*. 885 cm^{-1} band is considered negligible,[18] and therefore this band is taken as part of the contribution of $Mo_2O_7^{2-}$ dimers to the infrared spectrum. Since the extinction coefficients of the various units are not known, we distribute the intensity of the band at *ca*. 400 cm^{-1} equally between $Mo_2O_7^{2-}$ and MoO_6^{6-} species (Table 5), noting that this assumption does not influence the results presented in this section. Besides the above features, the sum of the intensities of bands at *ca*. 580 and 490 cm^{-1} is attributed to $Mo_2O_7^{2-}$ dimers, and the intensity of the band at *ca*. 680 cm^{-1} to MoO_6^{6-} octahedra.

The sum of $\Delta\epsilon_j$ (Table 1), or $\langle A \rangle_j$ (Table 2), of the above bands representing each structural unit is then normalized with respect to the corresponding total infrared activity in the range $\approx$250−1000 cm^{-1}. In this way, we obtain the normalized intensity, or relative contribution of each molybdate unit in the infrared range. As shown in Table 6, the two methods employed here give similar results. Therefore, it is found that ~68% of the infrared activity of the $x = 0.4$ glass arises from MoO_4^{2-} tetrahedra, while the corresponding activity of $Mo_2O_7^{2-}$ and MoO_6^{6-} species is approximately 22% and 10%, respectively. Increasing the CuI content ($x = 0.5$) induces a decrease of the contribution of MoO_4^{2-} tetrahedra to approximately 50% and the simultaneous increase of the activities due to $Mo_2O_7^{2-}$ and MoO_6^{6-} units to ~35% and ~15%, respectively. These findings are in accordance with the predictions based on eq 10, at least as far as trends are concerned.

The relative contributions of the molybdate units obtained (Table 6) can be used to estimate an equilibrium constant at constant pressure for the disproportionation reaction proposed in eq 10 as follows:

TABLE 6: Normalized Contribution of Molybdate Structural Units to the Infrared Activity in the 250−1000 cm^{-1} Range and Relative Equilibrium Constants for the Disproportionation Reaction (Eq 10) Calculated According to Eq 14. Results Obtained on the Basis of the Reflectance (Table 1) and Absorption Data (Table 2)[a]

xCuI·$(1-x)Cu_2MoO_4$	$x = 0.4$	$x = 0.5$
reflectance analysis		
MoO_4^{2-}	0.68 ± 0.01	0.52 ± 0.01
$Mo_2O_7^{2-}$	0.21 ± 0.01	0.33 ± 0.01
MoO_6^{6-}	0.11 ± 0.01	0.15 ± 0.01
K_r	$(3.5 \pm 0.6) \times 10^{-2}$	$(4.3 \pm 0.6) \times 10^{-1}$
absorption analysis		
MoO_4^{2-}	0.67 ± 0.01	0.49 ± 0.01
$Mo_2O_7^{2-}$	0.24 ± 0.01	0.37 ± 0.01
MoO_6^{6-}	0.09 ± 0.01	0.14 ± 0.01
K_r	$(3.5 \pm 0.7) \times 10^{-2}$	$(7.0 \pm 0.7) \times 10^{-1}$

[a] For details see text.

$$K_{eq} = X_O X_D^2 / X_T^5 \tag{11}$$

where X_T, X_D, and X_O are the mole fractions of MoO_4^{2-} tetrahedra (T), $Mo_2O_7^{2-}$ dimers (D), and MoO_6^{6-} octahedra (O), respectively. The fractions X_i (i = T, D, O) are related to the corresponding normalized infrared intensity, I_i, by

$$X_i = I_i/\alpha_i \tag{12}$$

where α_i is the normalized absorption coefficient of species i.[25] Equations 11 and 12 are combined to give:

$$K_{eq} = \left(\frac{\alpha_T^5}{\alpha_O \alpha_D^2}\right)\frac{I_O I_D^2}{I_T^5} \tag{13}$$

If the normalized absorption coefficients α_i are independent of composition and temperature we can define a constant K_α by $K_\alpha = \alpha_T^5/(\alpha_O\alpha_D^2)$, and rewrite eq 13 in the form:

$$K_r = \frac{K_{eq}}{K_\alpha} = \frac{I_O I_D^2}{I_T^5} \tag{14}$$

In the above expression, I_i denotes the normalized contribution of molybdate species i tabulated in Table 6. Thus, a relative equilibrium constant, K_r, can be evaluated in terms of eq 14. The results are included in Table 6 as a function of CuI content and the method used for infrared data analysis.

Considering the approximations made, it is found that K_r of a specific glass is independent of the method employed to analyze the data. Nevertheless, it is also shown in Table 6 that K_r increases by more than an order of magnitude as the CuI content increases from $x = 0.4$ to $x = 0.5$. To understand this trend we note that in general K_r depends on both pressure and temperature and reflects the state of glass structure arrested at the fictive temperature. Since the present glasses were prepared under identical quenching conditions, K_r will depend only on the fictive temperature at which the structure of the supercooled liquid was "frozen" into the glassy state. Fictive temperatures for these glasses are not known, but the glass transition temperature, T_g, was found to decrease upon increasing CuI content.[8] Specifically, T_g is 132 °C for $x = 0.4$ and 126 °C for $x = 0.5$. Therefore, the structure of the $x = 0.5$ glass was "frozen" in at a lower temperature than the structure of the $x = 0.4$ glass. This temperature lowering is obviously the reason for the larger K_r value of $x = 0.5$ glass. In an exactly analogous manner, eq 10 was found to shift to the right upon increasing the pressure (at constant temperature) at which a silver iodomolybdate melt was vitrified.[35]

The findings of this work regarding the effect of CuI on the molybdate structure, as well as the previous findings on the effects of AgI on the oxyanion glass matrix,[17,18,35,36,37] show clearly that these relatively inert halide salts affect glass structure in a rather indirect way. Increasing the amount of the halide salt causes the decrease of T_g, and presumably the decrease of the fictive temperature at which the structure of the supercooled liquid is arrested into the glassy state. This temperature decrease affects directly the value of the constant for the chemical equilibrium that describes a particular oxyanion system in the liquid state. For molybdate glasses, the spectroscopic data show that eq 10 is adequate to describe the oxyanion system. For AgI-doped borate glasses of relatively low metal oxide contents, like the diborates, the following chemical equilibrium was found to account for the borate structure:

$$B\text{ø}_2O^- \rightleftarrows B\text{ø}_4^- \tag{15}$$

where ø denotes an oxygen atom bonded to two boron atoms, and O^- is a nonbridging oxygen.[16,17] As the glass transition temperature decreases upon increasing the amount of AgI, the system responds by shifting equilibrium[15] to the right. This type of chemical restructuring in the liquid state was found to be the case in AgI-containing superionic borate glasses.[16,17,36,37]

4.3. Far-Infrared Spectra and the Nature of Cu^+ Ion Hosting Sites. The far-infrared (FIR) region of the measured spectra could be satisfactorily fitted with a minimum number of three component bands centred at *ca*. 60, 110, and 180 cm^{-1} (Tables 1 and 2). The previous study of xAgI·$(1-x)Ag_2MoO_4$ glasses showed that the far-infrared spectra could be best deconvoluted into three bands at *ca*. 50, 95, and 135 cm^{-1}.[18] These bands were assigned to Ag^+ ion oscillations in oxide (50 and 135 cm^{-1}) and iodide (95 cm^{-1}) environments. If we assume that the reduced mass of cation-site vibration can be approximated by the bare cation mass[16] and that the force constant of the corresponding modes of Cu^+ and Ag^+ motion remains nearly constant, then the frequencies of Cu^+-site oscillations should be proportional to those of Ag^+ ions with the proportionality factor being equal to $(m_{Ag}/m_{Cu})^{1/2} \approx 1.3$. On these grounds, it is reasonable to attribute the bands of the CuI-containing glasses at *ca*. 60 and 180 cm^{-1} to vibrations of Cu^+ ions in oxide environments and that at *ca*. 110 cm^{-1} to vibrations of Cu^+ ions in iodide sites. It should be noted that the band at *ca*. 180 cm^{-1} could contain some contribution from the rotation of MoO_4^{2-} anions[29] and from the bending vibration of Mo−O−Mo bridges of $Mo_2O_7^{2-}$ dimers.[38]

Crystalline CuI exhibits strong infrared absorption at 124 cm^{-1}, which arises from the vibration of Cu^+ ions against their tetrahedral iodide sites.[39] The present result, that the corresponding Cu^+ vibration in the $x = 0.4$ and $x = 0.5$ glasses appears at a lower frequency (∼110 cm^{-1}), is suggestive of distorted Cu iodide sites in the glass and/or of a small degree of aggregation of these sites into CuI-like pseudophases. In addition, at the interfaces between the Cu iodide sites and the oxyanion matrix it is possible to have some mixed coordination spheres where copper ions are coordinated with oxide and iodide anions.[18] The results of this study concerning the formation of disordered Cu iodide sites are in general agreement with the results of the anomalous X-ray scattering which have suggested a coordination environment of I^- around Cu^+ ions similar to that in molten CuI.[14] Comparison with analogous findings in AgI-containing glasses[18] suggests that the establishment of iodide sites hosting the charge carrier metal ions is a common characteristic of this type of superionic glasses. Thus, the early proposition[3] for the formation of conduction pathways along the metal iodide domains finds support from the present results.

TABLE 7: Densities, d, Molar Volumes, V_{mol}, Concentrations of Cu^+ Ions in Oxide, N_{Cu-O}, and Iodide Sites, N_{Cu-I}, and Corresponding Effective Charges in $xCuI\cdot(1-x)Cu_2MoO_4$ Glasses[a]

$xCuI\cdot(1-x)Cu_2MoO_4$	$x = 0.4$	$x = 0.5$
d (g cm^{-3})[b]	5.35 ± 0.01	5.30 ± 0.01
V_{mol} (cm^3 mol^{-1})	46.43 ± 0.08	45.04 ± 0.08
N_{Cu-O} (10^{28}/m^3)	1.557 ± 0.003	1.337 ± 0.002
N_{Cu-I} (10^{28}/m^3)	0.519 ± 0.001	0.669 ± 0.001
	0.56 ± 0.01(R)	0.74 ± 0.01 (R)
q_{Cu-O} (e)		
	0.58 ± 0.01(A)	0.76 ± 0.01 (A)
	1.00 ± 0.01 (R)	0.92 ± 0.01 (R)
q_{Cu-I} (e)		
	0.77 ± 0.01(A)	0.78 ± 0.01 (A)

[a] Note that by (R) and (A) are designated effective charges calculated by means of eq 16 and 17, respectively. [b] Reference 8.

It has been shown in previous works that the study of FIR profiles can yield useful information about effective ionic charges (see ref 16 and references therein). This is of particular interest in the present case, considering the questions about the formal oxidation state of copper mentioned in the Introduction. This study offers the opportunity to calculate effective charges by two independent methods and compare the results. The relevant equations are

$$\Delta\epsilon_j\nu_j^2 = \frac{1}{4\pi^2c^2e_0}\left(\frac{\epsilon_\infty+2}{3}\right)^2\frac{N_j}{m_{eff}}q_{eff}^2 \qquad (16)$$

$$\langle A\rangle_j = \frac{1}{4c^2e_0}\left(\frac{\epsilon_\infty+2}{3}\right)^2\frac{N_j}{n_jm_{eff}}q_{eff}^2 \qquad (17)$$

where N_j is the concentration of ions with effective charge q_{eff}; m_{eff} is the effective mass of vibration; n_j is the index of refraction at the frequency of the absorption maximum; e_0 is the permittivity of free space and c is the speed of light.[20,21] The high-frequency dielectric constant of glasses, ϵ_∞, was determined by the fitting procedure (Table 1), while m_{eff} was approximated by the mass of copper. The concentrations of copper cations in the oxide and iodide environments were calculated using density data (Table 7). Expressing the glass formula as $xCuI\cdot(1-x)Cu_2MoO_4$ and assuming that all copper cations introduced by CuI occupy iodide sites, the relevant concentrations can be written as follows:

$$N_{Cu-O} = \frac{2(1-x)}{V_{mol}}N_A \qquad N_{Cu-I} = \frac{x}{V_{mol}}N_A \qquad (18)$$

where N_{Cu-O} is the total concentration of copper ions in oxide environments and N_{Cu-I} is their concentration in iodide environments, V_{mol} is the glass molar volume, and N_A is Avogadro's number. The obtained concentrations of copper cations in the oxide and iodide environments are given in Table 7.

The spectroscopic parameters ($\Delta\epsilon_j$, ν_j and $\langle A\rangle_j$, n_j) of the ~110 cm^{-1} band were used to calculate the effective charge of copper ions in iodide sites, q_{Cu-I}. The corresponding parameters of bands at *ca*. 60 and 180 cm^{-1} were considered together to obtain an *average* effective charge of copper ions in oxide sites, q_{Cu-O}, by neglecting contributions to the ~180 cm^{-1} band other than the vibrations of copper ions in oxide sites. The effective charges were calculated by employing eqs 16 and 17 and are given in Table 7. The results show clearly that the formal oxidation state of Cu cations in these glasses is +1, in agreement with results of XPS studies on similar CuI-containing superionic glasses.[13,40] Thus, it is concluded that the preparation procedure employed in this work has resulted in glasses containing only cuprous ions.

The fact that the effective charges obtained are on the average less than +1 is an indication of some degree of covalency in the interactions between Cu^+ ions and their hosting sites.[41] Comparison between the effective charges of cuprous ions in iodide and oxide sites of the same glass suggests that this degree of covalency is greater in the oxide than in the iodide sites. The covalent character of such interactions is expected to be maximum in pure cuprous oxide, Cu_2O. Indeed, the effective charge of cuprous ions in this oxide was found to be 0.29e.[42] The data in Table 7 suggest that the Cu−site interactions in the oxide sites acquire more ionic character upon increasing CuI content. This is another manifestation of the structural rearrangement in the oxyanion matrix induced by CuI, as seen from the consideration of the mid-infrared spectra.

The effective charge of cuprous ions in crystalline CuI can be estimated using $\nu_j = 124$ cm^{-1}, $\epsilon_0 = 6.50$, $\epsilon_\infty = 4.85$[39,43] and $d = 5.62$ g/cm^3,[44] and approximating m_{eff} by the mass of copper. For one resonance only eq 6 gives $\Delta\epsilon_j = \epsilon_0 - \epsilon_\infty = 1.66$ and application of eq 16 results in an effective charge equal to 0.60e. The fact that this effective charge for crystalline CuI is smaller than the corresponding charges found in this work (see Table 7) gives additional evidence for the disordered nature of the cuprous iodide sites in the molybdate glasses.

5. Conclusions

In the present work we have studied by infrared reflectance spectroscopy superionic molybdate glasses containing CuI, with the purpose of investigating (a) the coordination state of the glass forming molybdenum cations, (b) the influence of CuI on the structure of the oxyanion matrix, and (c) the nature of sites occupied by copper ions and their oxidation state.

The two methods applied to analyze the data, i.e., the Kramers−Kronig inversion of reflectance and the fitting of reflectance according to classical dispersion theory, gave very similar results. In particular, the analysis of the mid-infrared spectra, combined with group theoretical considerations, showed that molybdenum exists in these glasses in fourfold and sixfold coordinations with oxygen atoms. Molybdate tetrahedra are present as monomers, MoO_4^{2-}, and dimers, $Mo_2O_7^{2-}$, while molybdate octahedra are in the form of isolated species, MoO_6^{6-}. The presence of the three kinds of molybdate structural units was described in terms of a disproportionation equilibrium, and a relative equilibrium constant was determined. The value of this constant was found to depend on the amount of CuI in the glass. This indirect influence of CuI on the glass structure was discussed in terms of its effect on the glass transition and fictive temperature at which the supercooled liquid is frozen into the glassy state. It is noted, however, that the majority species are the MoO_4^{2-} tetrahedra, while the $Mo_2O_7^{2-}$ dimers and the MoO_6^{6-} octahedra remain the minority species. The presence of $MoO_{4/2}O_2^{2-}$ type octahedra, containing four bridging and two nonbridging oxygen atoms, was excluded on the basis of the present mid-infrared spectroscopic results.

The study of the far-infrared spectra indicated that copper ions occupy two oxide- and one iodide-like site in the glass. The frequencies of Cu^+ ion vibrations against these sites were found to scale with those of Ag^+ ions in the analogous AgI-containing molybdate glasses.[18] Comparison with Cu^+−site interactions in crystalline CuI, suggests the disordered nature of the CuI microdomains in these glasses. The calculation of the effective charge of copper in oxide and iodide sites showed that copper ions are present only in the +1 oxidation state, and that their interactions with the sites are relatively more covalent in the oxide sites.

Acknowledgment. This work was supported by the Greek General Secretariat for Research and Technology through the PENED Program (grant No. 1065/95), by a Grant-in-Aid for Scientific Research from the Ministry of Education, Science, Sports and Culture of Japan (No. 08229240), and by the Proposal-Based Advanced Industrial Technology R&D Program from the New Energy and Industrial Technology Department Organisation (NEDO, Japan). C.P.V. and E.I.K. are very grateful to Drs. J. Kapoutsis and I. Koutselas for their help with spectral measurements and the setup of the minimization procedure used in this work, and to Dr. G. D. Chryssikos for helpful discussions.

References and Notes

(1) Ingram, M. D. *Phys. Chem. Glasses* **1987**, *28*, 215.
(2) Angell, C. A. *Annu. Rev. Phys. Chem.* **1992**, *43*, 693.
(3) Minami, T. *J. Non-Cryst. Solids* **1985**, *73*, 273.
(4) Souquet, J. L. *Solid State Ionics* **1988**, *28*−*30*, 693.
(5) Rousselot, C.; Malugani, J. P.; Mercier, R.; Tachez, M.; Chieux, P.; Pappin, A. J.; Ingram, M. D. *Solid State Ionics* **1995**, *78*, 211.
(6) Bartholomew, R. F.; Dorfield, W. G.; Murphy, J. A.; Pierson, J. E. Stookey, S. D.; Tick, P. A. U.S. Patent No. 4 226, 628 (1980).
(7) Liu, C.; Angell, C. A. *Solid State Ionics* **1984**, *13*, 105.
(8) Machida, N.; Chusho, M.; Minami, T. *J. Non-Cryst. Solids* **1988**, *101*, 70.
(9) Machida, N.; Minami, T. *J. Am. Ceram. Soc.* **1988**, *71*, 784.
(10) Machida, N.; Shinkuma, Y.; Minami, T. *Solid State Ionics* **1991**, *45*, 123.
(11) Sidhu, K. S.; Sekhom, S. S.; Chandra, S. *Phys. Chem. Glasses* **1992**, *33*, 212.
(12) Mika, M.; Sasek, L.; Rada, M. *Chim. Chronica, New Ser.* **1994**, *23*, 239.
(13) Minami, T.; Tatsumisago, M.; Machida, N. *Chim. Chronica, New Ser.* **1994**, *23*, 227.
(14) Saito, M.; Sugiyama, K.; Matsubara, E.; Jacob, K. T.; Waseda, Y. *Mater. Trans. JIM* **1995**, *36*, 1434.
(15) Kamitsos, E. I.; Patsis, A. P.; Karakassides, M. A.; Chryssikos, G. D. *J. Non-Cryst. Solids* **1990**, *126*, 52.
(16) Kamitsos, E. I.; Patsis, A. P.; Chryssikos, G. D. *J. Non-Cryst. Solids* **1993**, *152*, 246.
(17) Kamitsos, E. I.; Kapoutsis, J. A.; Chryssikos, G. D.; Patsis, A. P. *Bol. Soc. Esp. Ceram. Vid.* **1992**, *31*−*C4*, 403.
(18) Kamitsos, E. I.; Kapoutsis, J. A.; Chryssikos, G. D.; Hutchinson, J. M.; Pappin, A. J.; Ingram, M. D.; Duffy, J. A. *Phys. Chem. Glasses* **1995**, *36*, 141.
(19) Jamnicky, M.; Znasik, P.; Tunega, D.; Ingram, M. D. *J. Non-Cryst. Solids* **1995**, *185*, 151.
(20) Stern, F. *Solid State Phys.* **1963**, *15*, 299.
(21) Born, M.; Huang, K. *The Dynamical Theory of Crystal Lattices*; Oxford University Press: New York, 1954.
(22) Spitzer, W. G.; Miller, R. C.; Kleinman, D. A.; Howarth, L. E. *Phys. Rev.* **1962**, *126*, 1710.
(23) Mitcell, D. L.; Bishop, S. G.; Taylor, P. C. *J. Non-Cryst. Solids* **1972**, *8*−*10*, 231.
(24) Tsu, D. V.; Lucovsky, G.; Davidson, B. N. *Phys. Rev. B* **1989**, *40*, 1795.
(25) Mysen, B. O. *Am. Mineral.* **1990**, *75*, 120.
(26) Hardcastle, F. D.; Wachs, I. E. *J. Raman Spectrosc.* **1990**, *21*, 683.
(27) Nakamoto, K. Infrared and Raman Spectra of Inorganic and Coordination Compounds; Wiley: New York, 1978; Part II pp 105−171.
(28) Clark, G. M.; Doyle, W. P. *Spectrochim. Acta* **1966**, *22*, 1441.
(29) Tarte, P.; Rulmont, A.; Liegeois-Duyckaerts, M.; Cahay, R.; Winand, J. M. *Solid State Ionics* **1990**, *42*, 177.
(30) Tarte, P.; Liegeois-Duyckaerts, M. *Spectrochim. Acta* **1972**, *28A*, 2029.
(31) Mitchell, P. C. H.; Trifivo, F. *J. Chem. Soc. A* **1970**, 3183.
(32) Dupuis, T.; Viltange, M. *Microchim. Acta* **1963**, 232.
(33) Ross, S. D. Inorganic Infrared and Raman Spectra; McGraw-Hill: London, 1972; Chapter 10.
(34) Blasse, G.; Corsmit, A. F. *J. Solid State Chem.* **1973**, *6*, 513.
(35) Pappin, A. J.; Ingram, M. D.; Hutchinson, J. M.; Chryssikos, G. D.; Kamitsos, E. I. *Phys. Chem. Glasses* **1995**, *36*, 164.
(36) Minami, T.; Ikeda, Y.; Tanaka, M. *J. Non-Cryst. Solids* **1982**, *52*, 159.
(37) Minami, T.; Shimizu, T.; Tanaka, M. *Solid State Ionics* **1983**, *9*−*10*, 9810.
(38) Michel, G.; Machiroux, R. *J. Raman Spectrosc.* **1983**, *14*, 22.
(39) Plendl, J. N.; Hadni, A.; Claudel, J.; Henninger, Y.; Morlot, G.; Strimer, P.; Mansur, L. C. *Appl. Opt.* **1966**, *5*, 397.
(40) Machida, N.; Matsuda, Y.; Shigematsu, T.; Nakanishi, N.; Minami, T. *Solid State Ionics* **1994**, *73*, 63.
(41) Duffy, J. A.; Chryssikos, G. D.; Kamitsos, E. I. *Phys. Chem. Glasses* **1995**, *36*, 53.
(42) O'Keeffe, M. *J. Chem. Phys.* **1963**, *39*, 1789.
(43) Potts, J. E.; Hanson, R. C.; Walker, C. T. *Solid State Commun.* **1973**, *13*, 389.
(44) *CRC Handbook of Chemistry and Physics*; West, R. C., Ed.; CRC Press, Inc.: Boca Raton, FL, 1983; Part B, p 90.